SUPPLEMENTARY INFORMATION

SI Experimental

Microfluidic chips. The general design of the PDMS chips used for capture is presented in Fig. S1: the main chamber has a triangular shape 13 mm in length and 2.6 mm at its maximum width, with an aperture angle of 13°. A bent channel (100 µm in width) connects the inlet of the main chamber to 3 fluid reservoirs. This geometry avoids that beads escape through the inlet in no-flow conditions. The outlet is placed on the opposite side of the chamber. The height of all structures is 50 µm. The chips are fabricated by standard casting of PDMS on a prefabricated mold prepared by micromilling. In order to ensure uniform surface properties on all faces, the PDMS block bearing the channels is bonded immediately following plasma treatment, onto a second flat PDMS film cast on a glass coverslip. A surface treatment with poly-dimethyl-acrylamide bearing epoxy function (E-PDMA)[1] was immediately applied by incubation for one hour in the channel of an aqueous solution of this polymer at a concentration of 0.25% (w/v), followed by rinsing with deionized water.

***Pressure and flow control*.** Inputs for sample and reagents were connected through PEEK tubes (50 µm inner diameter) to their respective sample and reagents reservoirs, and the source of fluid to the chip inlet was selected in an automated manner by flipper solenoid valves (Bürkert, 6604). Flow control was achieved thanks to a pressure controller (MFCS™, Fluigent) applying pressure to the sample and reagents reservoirs. A feedback given by a flowmeter (Flowell, Fluigent) connected to the output of the chip, under control of the dedicated software (FRCM, Fluigent), allowed flow at predefined flow rates. A PEEK tube, inner diameter 250 µm connected to this flowmeter could be directed to a waste reservoir, or to collection tubes for subsequent analysis (e.g. quantitation of capture efficiency, see below).

Capture efficiency. The protocol for evaluation of the capture efficiency was as follows (see also SI Fig. 1):

1. The whole system was filled with phosphate buffer saline (PBS) with 1% bovine serum albumin (BSA);

2. 10 µL of the initial suspension of anti-S*almonella* Dynabeads® (50 µg) were first washed in tube and then injected inside the chamber thanks to a pipette tip at the chamber outlet. A small magnet below the chip was used to guide the beads to the chamber during this loading step;

3. A NdFeB 1.47 T permanent magnet (N50, Chen yang Technologies) was placed at a distance of 2 mm from the bent channel, symmetrically aligned with the axis of the main chamber;

4. A sample volume of 50 µL was injected through one of the inlets at a flow-rate of 1 µL/min, except when stated otherwise in the text;

5. The beads were washed inside the chip after capture with 40 µL of PBS containing 1% BSA through a second inlet at a flow-rate of 1.5 µL/min;

6. Triplicate cell culture plating was performed with 50 µL aliquots of each of:

i: the initial sample reservoir;

ii: the total eluted volume collected in a tubing at the output of the chip during the capture step (Tygon© 500 µm-inner diameter, 60 cm-long, instead of the PEEK tube previously described between the output of the chip and the flowmeter);

iii: the beads flushed from the chip after the capture step.

Colonies were counted the following day and the capture rate was estimated as the ratio between captured bacteria (from plating of beads) and the addition of both captured and non-captured bacteria (non-captured meaning sample collected in Tygon© tube). This procedure was selected, rather than a reference to the initial number of bacteria spiked in the sample. The latter approach led to similar values in average, but with a higher dispersion, probably due to difficulties in evaluating accurately the absolute number of spiked bacteria, especially at low numbers.

***On-chip bacterial culture and amplification*.** The protocol for on-chip culture started as that previously described for capture efficiency evaluation, but diverged from step 6: culture was started by injecting lysogeny broth through inlet at 0.15 µL/min. The temperature was set at 37°C with the use of a glass slide coated with indium tin oxide (ITO) connected to a voltage controller (Eurotherm 3508) and feedback-regulated with the input from a thermocouple placed between the glass slide and the chip. For fluorescence measurements, time-lapse images were taken every minute with a Nikon Ti microscope and a CoolSNAP HQ2 camera.

For the direct detection of bed expansion, images were obtained by real-time recording of the bed by a low-cost camera (AM4013MZTL, Dino-Lite). The bed expansion was quantified from images stacks with a home-made software written in Image-J, taking as reference the position of the front of the bed before broth infusion, and measuring the positive displacement towards the output along the axis of the chamber.

***Bacteria strains and viable cell count*.** *Salmonella enterica* serovar Typhimurium ATCC14028 and the isogenic csgD mutant strain affected in biofilm formation were obtained from Françoise Norel's collection (Institut Pasteur). To monitor bed expansion the ATCC14024 strain was transformed by the pFPV25.1 (Ap^R) plasmid, to express green fluorescent protein (GFP)[2]. Quantification of bacteria was achieved by counting the total number of colony-forming units (cfu) grown onto Lysogeny broth (LB) agar from serial dilutions of the original sample and expressed as cfu/ml.

***Batch determination of population doubling time*.** The population doubling time of wild type and mutant bacteria strains was determined by measuring as a function of time the optical density (OD) of bacteria suspension in agitated flasks of LB kept at 37°C. The doubling time T is deduced from the slope of the log(OD) versus time. The result obtained this way is independent of the initial density of bacteria, and of the volume and intrinsic OD of the bacteria strain.

Deciphering the mechanism of bed expansion

Bed expansion could be due to different possible contributions, such as : (i) a direct steric effect, related to the volume occupied by the new bacteria, (ii) a modification of the bed hydrodynamics, through e.g. changes in adhesion or friction properties of the bacteria-loaded beads, or (iii) the formation of biofilms. In order discriminate between these possibilities, additional series of experiments were performed, using a wider range of bacteria concentrations in the initial sample, and mutant bacteria with modified adhesion and/or biofilm formation capabilities. The direct effect of bacteria volume was checked by injecting in the fluidized bed a highly concentrated solution of *S.* Typhimurium (10^8 cfu/ml), and following the bed expansion. In this case, the expansion starts immediately during the capture phase, without nutritious medium and heating of the chip (Supplementary Figure 2). The volume increase is proportional to the total number of injected bacteria. This indicates that the volume occupied by the bacteria can directly yield bed expansion without growth. Further, when bacteria are cultivated on-chip from this pre-expanded state, by flowing culture medium and heating the chip at 37°C, bed expansion continues readily (Supplementary Figure 2b), confirming the absence of a lag phase for culture, already suggested by the direct counting of fluorescent bacteria in the diluted regime.

The above experiments demonstrate a direct steric contribution of the captured bacteria to the bed expansion. This, however, does not preclude other contributions. In particular, numerous studies have shown that *Salmonella spp.* are capable of forming biofilms under certain conditions depending on substrate, pH, temperature or salinity [3,4]. Biofilm formation could affect the fluidized bed properties through different mechanisms, such as volume occupancy of the extracellular matrix, crosslinking, or screening of ligands. This was investigated by using a biofilm-defective mutant strain of *S.* Typhimurium, i.e. a knock-out mutant of the *csgD* gene involved in expression of both curli fimbriae (known to aid in biofilm formation, cell aggregation and cell adhesion [5]) and cellulose (a main constituent of *Salmonella*-produced biofilms [6]). To avoid any bias related to the doubling time of

bacteria, this time (needed to double the mutant population) was measured and shown to be close to that of the wild type (Supplementary Figure 3).

The bed expansion was similar to that obtained for the non-mutated strain, suggesting that the formation of biofilms does not play a significant role in the expansion phenomenon. Interestingly, it also indicates that adhesion and aggregation of bacteria have a marginal impact on bed expansion. Overall, these results emphasize the generality of the method, since it does not depend on some specific collective properties of cells, but merely on their intrinsic volume and proliferation capacity.

Estimating effective bacteria volume

The effective bacteria volume that best fit experimental data with the simple exponential growth model of expansion is $V_{bac} = 4.8x10^{-9}$ µL. Considering that the effective volume of bacteria in the bed must take into account steric effects due to the specific orientation of each bacterium, the length and shape of the flagella, the natural variation of volume of each bacteria during its growth, and genotypic and phenotypic differences between different strains in different conditions, it is difficult to provide an accurate "a priori" evaluation of a single bacterium steric exclusion volume. *Salmonella spp.* is a rod shaped bacteria with a diameter ranging from 0.7-1.5 µm and 2-5 µm in length with optimal growth condition of 37 ◦C. This yields an expected volume range between 1.4 and 7.5 $x10^{-9}$ µL [7,8]. The best fit effective volume obtained here, $V_{bac} = 4.8x10^{-9}$ µL, is thus well within the expected range.

Measurement of bacteria release from the fluidized be during the expansion phase

The release of bacteria from the fluidized bed during on-chip culture was evaluated, by collecting the fluid exiting the chamber and counting the released bacteria by serial dilutions and plating (Supplementary Figure 5).

During the early stages of growth medium perfusion, only a few bacteria leave the bed. Incidentally, this provides an additional proof of the high capture efficiency of the fluidized bed. Regarding our

growth model (Eq. 2 Main text) model, this part of the bed expansion curve should be well described by our model. More specifically, for the conditions evaluated (350+/-50 captured cfu) during the first two hours, the number of released bacteria does not increase, suggesting that most bacteria produced during the initial phase are recaptured on the beads. Bacteria start to be released in significant amounts after this time, and the released amount continuously increases afterwards. The experimental bed expansion deviates from the theory around 370 min. This corresponds to a bed expansion of about 1 mm, representing 60% of the initial bed volume. It is not surprising that such volume occupancy by bacteria starts to have a significant screening effect on the recapture of newly produced cells. This, combined with the fact that the release rate of cells continues to grow beyond this time point, suggests that the saturation of the bed growth, and the deviation of the effective growth from the model at long time, are both due to a saturation of the capture sites, and not to a loss of viability of the cells in the bed.

Additionally, to evaluate the release variability depending on the bacteria/ligand couple, experiments have been performed for *S*. Typhimurium with anti-*Salmonella* beads, *E. coli* O157:H7 with anti-*E. coli* beads, and *S.* Typhimurium with non-grafted magnetic beads (Carbocylic Acid Dynabeads®), all from the same initial bacteria concentration (2500+/-200 cfu, Supplementary Figure 6). The release of bacteria in the absence of antibodies was very low for all times. We did not observed any significant exponential increase as observed when specific antibodies are used. This suggests that any possible contribution to the expansion phenomena due solely to the mechanical trapping of bacteria is negligible, reinforcing the specific nature of our detection. Similarly to *S.* Typhimurium, an exponential release of bacteria was observed for *Escherichia Coli* when tested with its specific antibodies, the release of *E. coli* taking place slightly later, as expected from its moderately later expansion for a given concentration (see Fig. 4).

Elements of cost analysis

A detailed cost per analysis evaluation is difficult to achieve accurately at this stage, since this involves many non-technical aspects, but the technology carries several features favoring very low costs: As can be seen in Fig. S6, the design of the chips itself is extremely simple, it does not involve active sensors, electrodes, actuators or high resolution features, so the disposable part of the device can be mass produced in thermoplastics for a few cents per chip, by e.g. injection molding. The cost of biochemicals is also considerably reduced as compared to other techniques: the biological specificity and selectivity is carried onto the magnetic beads, avoiding the need to functionalize *in-situ* the chip. The latter process is a strong hindrance to industrialization, since it involves fluidic connection and processing of each individual chip during production, and it also implies a high consumption of antibodies. In contrast, magnetic beads can be functionalized in large quantities in batch processes, reducing costs and facilitating quality control. Functionalized magnetic carriers can be rather expensive, but the consumption of the fluidized bed device is reduced by a factor of 10 to 100 as compared to methods using beads-based capture in conventional batch format or as a pre-processing step. Finally, the method is also very cost-effective on the detection side, since it does not involve high-tech optics, expensive sensors or cameras, or micro-nano electrodes, and can be operated with a smartphone, webcam or optical designs typically costing a few $.

SI References

1 M. Poitevin, Y. Shakalisava, S. Miserere, G. Peltre, J. L. Viovy and S. Descroix, *Electrophoresis*, 2009, **30**, 4256–4263.

2 M. Rathman, N. Jouirhi, A. Allaoui, P. Sansonetti, C. Parsot and G. T. Van Nhieu, *Mol. Microbiol.*, 2000, **35**, 974–990.

3 S. K. Hood and E. A. Zottola, *Int. J. Food Microbiol.*, 1997, **37**, 145–153.

4 X. Shi and X. Zhu, *Trends Food Sci. Technol.*, 2009, 20, 407–413.

5 M. M. Barnhart and M. R. Chapman, *Annu. Rev. Microbiol.*, 2006, **60**, 131–147.

6 C. Latasa, A. Roux, A. Toledo-Arana, J. M. Ghigo, C. Gamazo, J. R. Penadés and I. Lasa, *Mol. Microbiol.*, 2005, **58**, 1322–1339.

7 M. Dworkin, S. Falkow, E. Rosenberg, K.-H. Schleifer and E. Stackebrandt, *The Prokaryotes: A Handbook on the Biology of Bacteria: Archaea. Bacteria: Firmicutes, Actinomycetes*, 2006.

8 K. L. T. M. G. Abatcha, Z. Zakaria, D. G. Kaur, *Adv. Life Sci. Technol.*, 2014, **17**.

Supplementary Figures

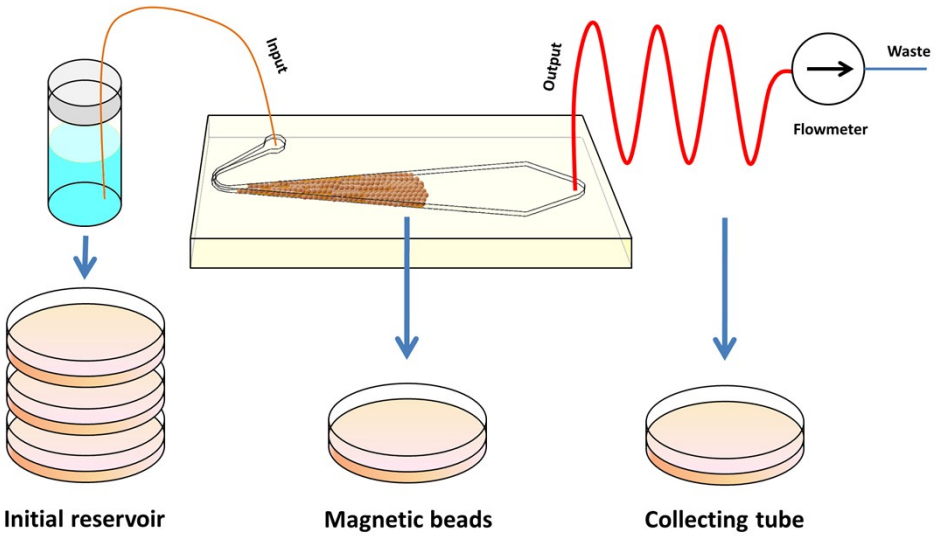

Supplementary Figure 8. *Protocol followed for the determination of the capture rate of the immune-extraction step: 50 µL of the initial sample were plated three times for average counting; magnetic beads were extracted from the chip after the washing step by high pressure flushing and immediately culture plated; a Tygon© reservoir was placed at the outlet and just before the flowmeter to collect 120 µL of output volume containing non-captured bacteria, the total volume also plated once.*

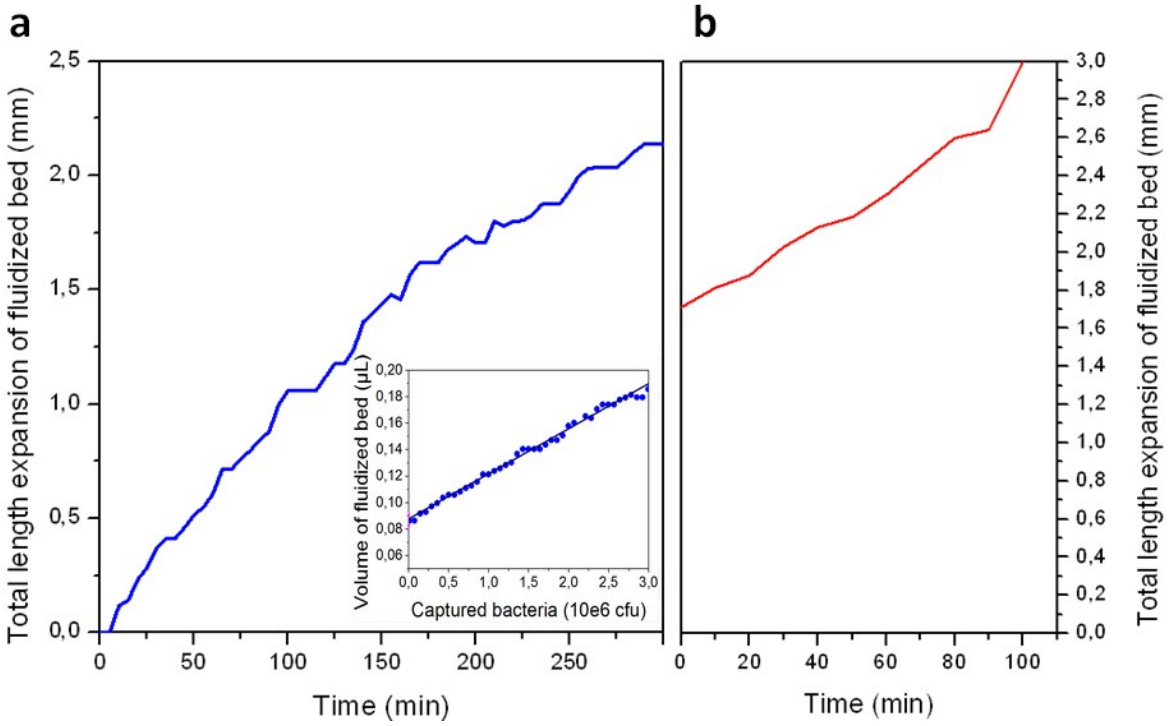

Supplementary Figure 2. *(a) Results of an experiment showing expansion of the fluidized bed during the capture step from a solution of S. Typhimurium at high concentration (10^8 cfu/ml). In this case, the flow rate during capture was 0.15 µL/min, as for the culture step to allow direct comparison of bed lengths. Note that the figure reports the length of the bed. The curve is not linear, because of the triangular shape of the chamber: upon lengthening of the bed, the length growth rate decreases because the bed progressively occupies parts of the chamber with a larger width. The volume increase, deduced by taking into account the triangular shape of the chamber is, within experimental error, linear in time within the number of injected bacteria (insert figure). (b) Expansion curve obtained during culture step, for a high concentration of initial salmonella (6.10^6 captured bacteria). In both figures the zero length reference corresponds to the size of the bed prior to any cell capture, at a flow rate of 0.15 µL/min.*

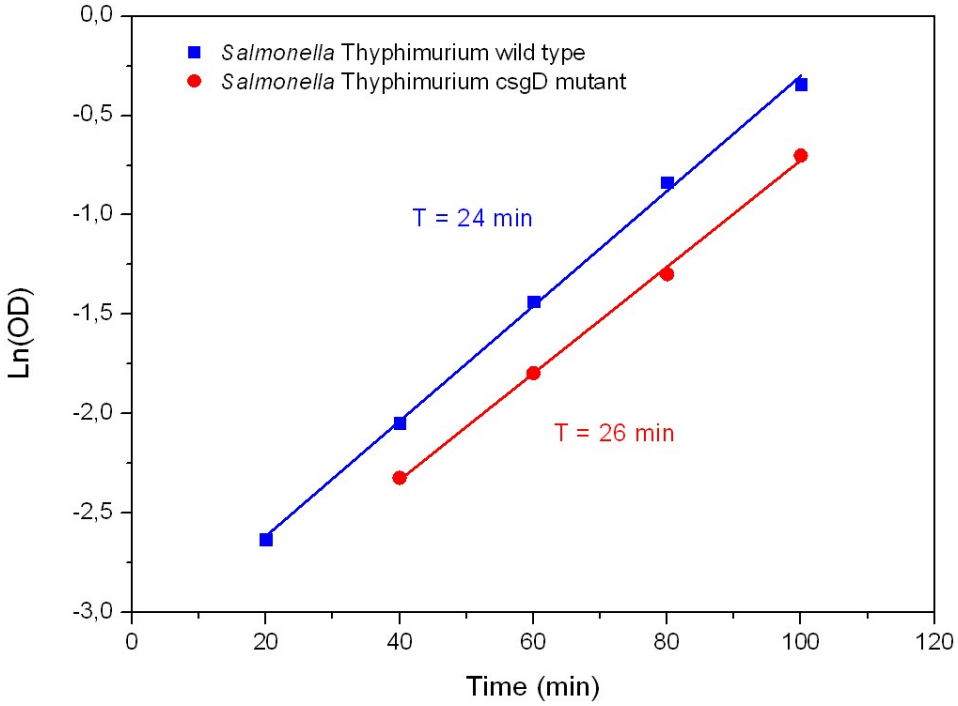

Supplementary Figure 3. *Exponential phase of growth curves obtained for the batch culture of S. Typhimurium and the csgD mutant. Medium was LB Broth and temperature 37°C. The calculated generation (doubling) times T are indicated for both strains.*

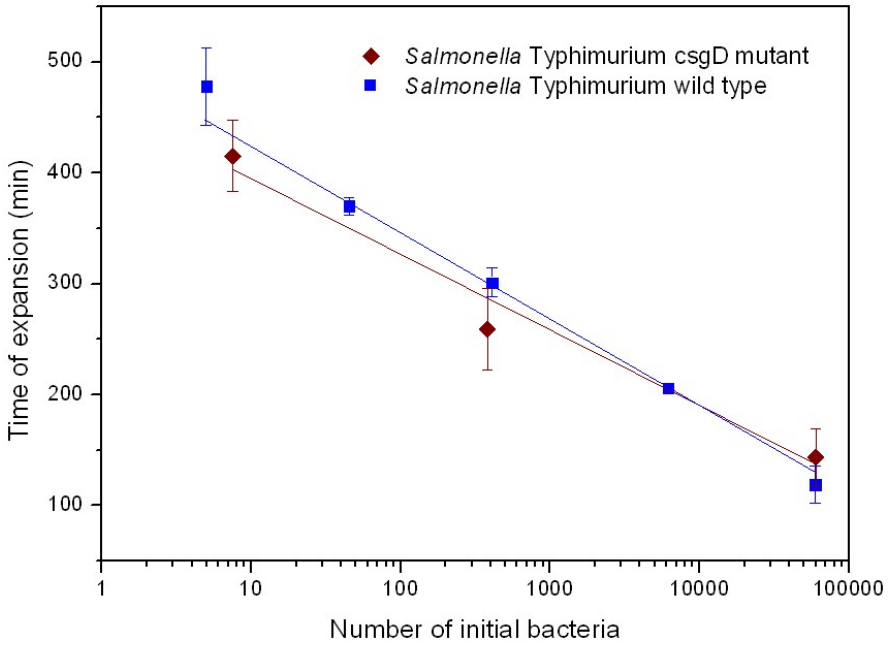

Supplementary Figure 4. *Expansion times (for threshold expansion of 200 µm, see article main text) obtained with the csgD mutant of S. Typhimurium affected in biofilm formation. No significant differences between the mutant and wild type expansion times.*

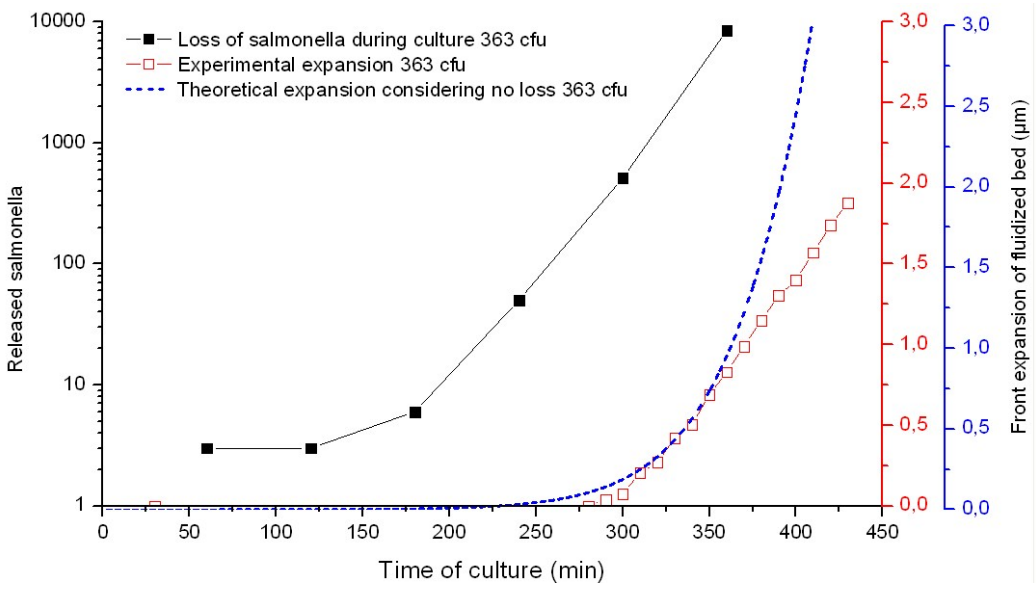

Supplementary Figure 5. *Number of released S. Typhimurium cells from the fluidized bed during the culture step (black squares), after capture from a 50 µl sample containing 350+/-50 cfu (measured by colony plating). Each square represents the bacteria released during the previous hour. The bed expansion for the same experimental conditions is plotted as red squares (red vertical scale), the model's prediction as a blue dashed line (blue vertical line).*

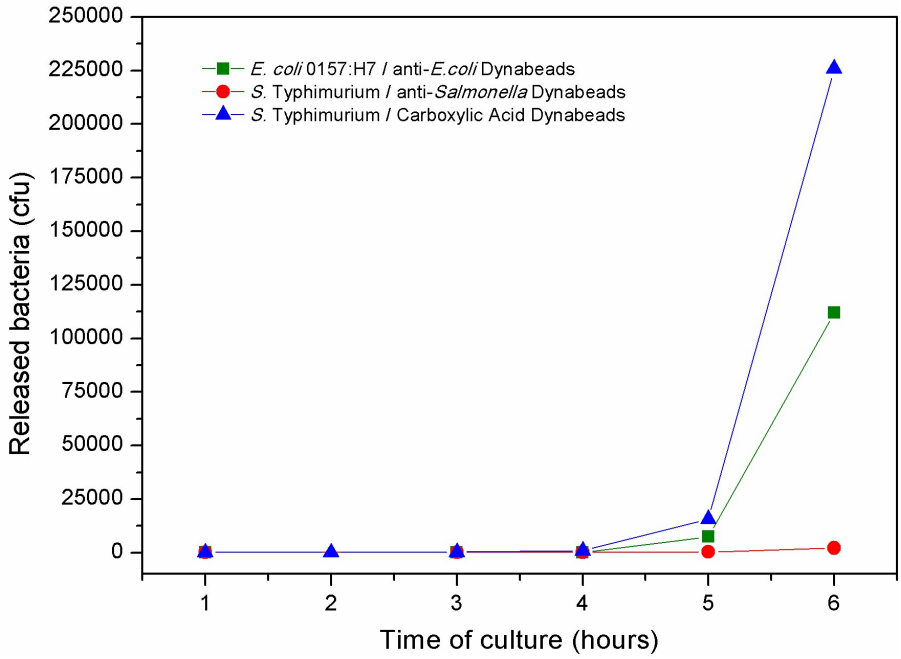

Supplementary Figure 6. *Number of released bacteria from the fluidized bed during culture for an initial 50 µL sample containing 2500+/-500 cfu (measured by colony plating), similar to the previous figure. In this case the release of S. Typhimurium (blue rectangles) is compared to the same case with S. Typhimurium with non-grafted bare beads (M-270 Carboxyl Acid Dynabeads, red rectangles) and E. coli 0157:H7 with anti-E.coli 0157-H7 Dynabeads (green squares).*

Video legends

Supplementary Video 1 : Bright field real-time video showing steady-state beads recirculation in the full chamber, at a flow rate of 90 µl/h.

Supplementary Video 2 : Real-time video in conditions identical to those of Supplementary Video 1, zooming on the downstream region of the fluidized bed to focus on beads longitudinal organization and recirculation.

Supplementary Video 3: Real time video of the fluidized bed exit, during flow of unskimmed UHT milk at a flow rate of 60 µl/h. Numerous fat droplets can be seen as light grey dots escaping from the bed and flowing from right to left, while the vast majority of the magnetic particles (black dots) are retained.

Supplementary Video 4: Time lapse video of the bed expansion during perfusion of nutritious medium at 0.15µl/mn, after bacteria capture at 1 µl/mn from a sample containing ~8000 bacteria. Elapsed time on upper left.

Supplementary Video 5: Real-time zoom on the terminal part of the fluidized bed after capture and culture of GFP-fluorescent S. Typhimurim , in the bed expansion saturation zone: new bacteria are continuously produced, and can be seen as individual green dots escaping the fluidized bed border.